J. Micromech. Microeng. **17** (2007) 1567–1574 doi:10.1088/0960-1317/17/8/020

A microengineered alignment bench for a nanospray ionization source

R R A Syms[1], H Zou[1], M Bardwell[2] and M-A Schwab[2]

[1] Optical and Semiconductor Devices Group, Electronic and Electrical Engineering Department, Imperial College, Exhibition Road, London SW7 2AZ,
[2] Microsaic Systems Ltd, GMS House, Boundary Road, Woking, Surrey, UK

E-mail: r.syms@ic.ac.uk

Received 9 March 2007, in final form 14 May 2007
Published 13 July 2007
Online at stacks.iop.org/JMM/17/1567

Abstract
A microengineered alignment bench for a nanospray ionization system is described. The bench combines a V-groove mount for a capillary-based nano-ESI source with an extraction electrode and allows accurate axial and transverse alignment of the capillary. An input channel and plenum for nebulizer gas are also demonstrated. The structure is formed in two halves, which are assembled by stacking. Electrically conducting features are constructed by crystal plane etching, deep reactive ion etching and metallization of silicon, while the insulating base is formed in a photopatterned plastic. Low voltage (about 850 V) positive ion emission is demonstrated using commercial nanospray (15 μm ID) capillaries, with total ion currents >10 nA. The structures are robust, and can survive voltages >1 kV and immersion in common solvents. Mass spectrometry is carried out using a commercial atmospheric pressure ionization instrument, and high signal stability is demonstrated.

1. Introduction

Since the pioneering work of Dole [1], Fenn [2] and Wilm [3], electrospray ionization mass spectrometry (ESI-MS) has become a key analytical tool of biochemistry, especially when combined with liquid chromatography (LC) or capillary electrophoresis (CE). Early ESI-MS systems had capillaries with inside diameters (IDs) of ≈100 μm, flow rates of 0.5–5 μL min^{-1} and extraction voltages of 2.5–4 kV. A steady reduction in flow rates has led to the development of nanospray systems based on tapered capillaries with IDs down to ≈5 μm and operating in the low nL min^{-1} range [4, 5]. Nanospray systems are compared with electrospray in [6, 7] and reviewed in [8–10].

Electrospray was studied in the early 1900s by Zeleny [11]. The phenomenon depends on physical properties (the conductivity σ, dielectric constant ε and surface tension γ of the liquid), geometric properties of the ESI source and set-up (the capillary internal radius R and the capillary-electrode separation D) and operational parameters (the applied voltage V and flow rate Q). In a classical paper, Taylor modelled electrospray from a liquid cone with a fixed semi-angle of 49.3° [12]. Later studies have pointed out the theoretical modifications needed due the spray jet [13–15] and surface charge [16, 17]. There is reasonable agreement amongst predictions for scaling laws, namely that the threshold voltage V_T for cone formation varies as $V_T \sim (\gamma D/\varepsilon_0)^{1/2}$ [3], the ion current I varies as $I \sim (\gamma Q\sigma/\varepsilon)^{1/2}$ [17], while the radius r of the sprayed droplets varies as $r \sim (Q\varepsilon\varepsilon_0/\sigma)^{1/3}$ [16]. Decreasing the capillary-electrode separation decreases voltages, while decreasing the flow rate alters the droplet size and subsequent fission processes, and allows efficient formation of ions with a high charge-to-mass ratio.

Nanospray capillaries are well understood, and may be used with or without a gas flow to promote nebulization. They are generally formed in fused tapered silica [18], have been investigated uncoated (with an internal contact) [4, 19] or coated with layers of Au [20], SiO_x-coated Au [21], polyaniline [22] or graphite [23]. The stability and analytical performance of these coatings is compared in [24]. One consequence of the low flow is the difficulty of maintaining a stable spray, and low-cost nanospray components can require complex alignment and monitoring systems [25].

Increasingly, attempts are being made to integrate the components of CE-ESI systems. These efforts have concentrated on the integration of the spray nozzle with other

fluidic elements. Ramsey showed that a spray could be drawn from a glass chip containing an etched capillary [26], and Figeys combined a nozzle with sample and buffer reservoirs [27]. One issue with glass substrates is their hydrophilic nature, which allows the Taylor cone to spread as the flow rate rises. Wetting may be controlled using hydrophobic polymers. Licklider has demonstrated a parylene-coated silicon source [28], and a large number of very similar emitters have been made in different polymers including PDMS [29], PMMA [30], polycarbonate [31] and cyclo olefins [32]. Some authors have used closed channels, while others have used nib-shaped or open channels [32–34]. Metal [35] and carbon fibre [36, 37] emitters have also been investigated. Devices with in-plane flow have been developed as one-dimensional (1D) arrays, and devices with through-wafer flow as 2D arrays [38–40]. A device with a microfabricated nebulizer was recently demonstrated [41]. Microfluidic devices for CE-ESI-MS are reviewed in [42].

In this paper, we take a different direction and consider the application of integration technologies to low-cost alignment of nanospray systems, particularly by combining a capillary mount with a closely spaced ion extraction electrode and a nebulizer to form a complete electrospray ion gun. Silicon microengineering has long been used to construct miniature optical benches, exploiting crystal plane etching [43, 44] to form V-shaped alignment grooves for optical fibre connectors [45] and transceivers [46]. Clearly, since capillary emitters have similar forms and dimensions to fibres, it should be possible to form alignment systems for the ion optics in nanospray. However, several key technologies are needed for this alternative application.

In the past, the feature-shape constraints of crystallographic etching made it impossible to combine V-grooves with suitable electrodes. High-density plasma etching has removed this restriction, allowing arbitrary shapes to be etched vertically in silicon [47]. Similarly, electro-deposited resist now allows non-planar surfaces to be patterned [48]. Finally, an epoxy-based photoresist, SU-8, has provided a rugged photopatterned plastic [49]. As we show here, it can provide electrical insulation capable of surviving high on-chip voltages. Finally, wafer stacking and bonding has allowed the construction of diaphragm electrodes set up normal to the wafer plane, for example in a miniature quadrupole mass spectrometer [50].

Here, we show how these techniques can be combined to construct a chip-based alignment bench for nanospray capillaries. The microbench provides a protective environment for the capillary tip, and allows spray to be initiated at low and consistent voltages using a self-aligned extraction electrode. Nebulization is achieved using an on-chip gas delivery system. The design concept and fabrication details are given in section 2, and characterization and the results of experiments carried out using the chip alone and with a commercial ESI mass spectrometer are presented in section 3. It is shown that high signal stability can be achieved, with weak dependence on the position of the nanospray source. Conclusions are drawn in section 4.

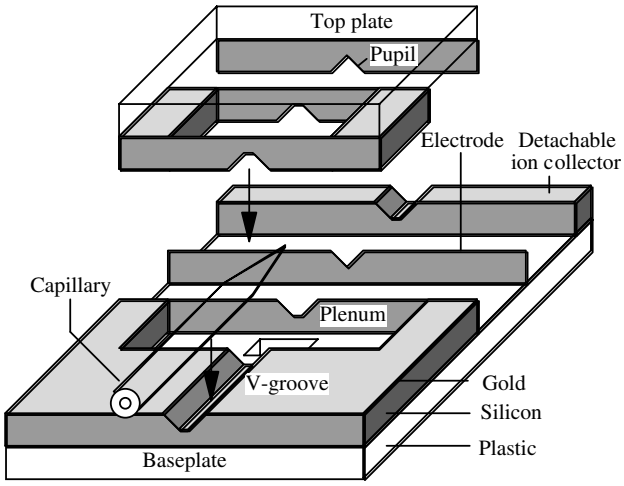

Figure 1. Principle of a microengineered nanospray alignment bench.

2. Design and fabrication

2.1. General construction

Figure 1 shows the construction of the microengineered nanospray bench. The system is a stacked assembly of two chips. The base plate carries an alignment groove for a capillary, a partial extraction electrode, a gas inlet and plenum chamber and (in the test structure shown) a detachable ion collector. The top plate also carries a partial electrode. The electrodes and alignment features are formed in silicon, and the underlying structure in plastic.

Crystallographic etching of (1 0 0) oriented Si [43] is used to form V-shaped grooves and indentations in the partial electrodes, as shown in figure 2(*a*). Etching may be carried out using standard solutions such as potassium hydroxide (KOH), using SiO_2 as a mask [44]. The exposed (1 1 1) crystal planes lie at an angle $\theta = \cos^{-1}(1/\sqrt{3}) = 54.73^\circ$ to the surface, and a groove of width $W_g = d/\sin(\theta) = d\sqrt{(3/2)}$ will seat a capillary of diameter $d = 2R$ with its axis lying in the wafer plane. An over-etched groove will be self-terminating at its apex. When two etched substrates are stacked together, the combined indentations form diamond shaped pupils, whose width W_p and height $H_p = W_p \tan(\theta) = W_p\sqrt{2}$ may also be controlled using variations in an initial groove width. Six-sided pupils more closely approximating circles may be formed from under-etched grooves.

A groove of sufficient depth to seat a standard nanospray capillary (about 320 μm OD) must be at least 160 μm deep. Once the grooves have been etched, the wafer surface is highly non-planar, and the conventional spin-coating methods of depositing photoresist for any subsequent lithography can no longer be used. Conformal resist layers may, however, be deposited electrophoretically on a metal seed layer [48]. Such layers have thicknesses that are less controllable than spin-coated layers, and may not be patterned with high-resolution at large depths. However, they are sufficient for many structures with surface topographies several hundred microns deep.

Plasma etching is used to define the major silicon blocks and the electrode layout. Near-vertical etching of silicon may be carried out at high-rates (1–4 μm min^{-1}) in an inductively

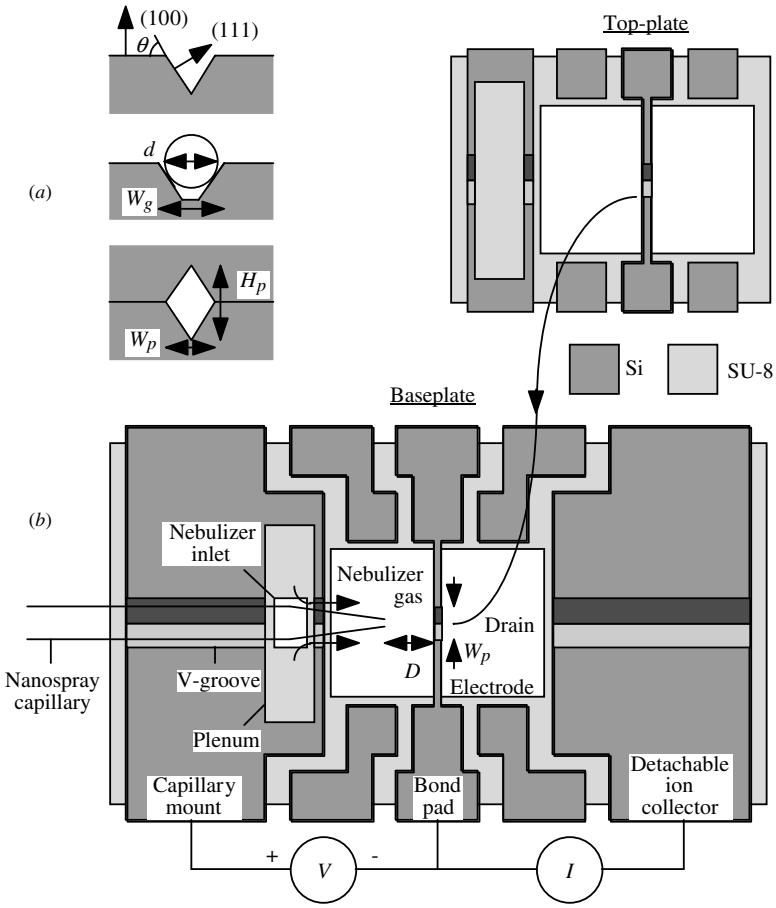

Figure 2. Layout of a microengineered nanospray alignment bench: (*a*) in section and (*b*) in plan.

coupled plasma, using the cyclic process developed by Robert Bosch GmbH, which involves alternating steps of passivation using C_4F_8 and etching using SF_6 [47]. Photoresist and SiO_2 are both suitable mask materials, and selectivities of >60:1 are routinely obtained, allowing full wafer depths (e.g. 450 μm for a 100 mm diameter wafer) to be etched using photoresist mask layers ≈10 μm thick.

2.2. Die layout

Figure 2(*b*) shows a detailed die layout. The silicon layer contains a capillary mount, an extraction electrode (or, more generally, multiple electrodes) and associated bond pads, a plenum chamber with a nebulizer orifice, and a detachable ion collector. The plastic layer beneath contains a gas inlet channel to the plenum and a fluid drain beneath the spray region. The plenum is designed to create a co-axial gas flow by leakage through the clearance between the capillary and the V-groove, so that nebulization can take place on-chip in a small, well-defined volume. Clearly, the overall scheme offers scope for considerably more complex arrangements of electrodes and gas and liquid channels.

2.3. Microfabrication process

The device is fabricated using a planar process based on conventional silicon wafers. Figure 3 shows the main steps, which involves three masks: mask 1—optical component definition, mask 2—plastic substrate definition, and mask 3—electrode definition. Mask 1 is first used to define all the V-shaped alignment and electrode pupil features, which are transferred into the silicon by crystallographic etching (step 1). Different OD capillaries can be accommodated by altering the width of the mounting groove on this mask. The wafer is turned over, and mask 2 is then used to define all the underlying features in photosensitive plastic (step 2). The wafer is turned over again, metallized, and patterned with mask 3 (step 3), and the electrode features are transferred right through the silicon substrate by deep reactive ion etching. Finally, the dies are detached from the wafer and arranged as wirebonded stacks on small PCBs (step 4). Nanospray capillaries are then inserted into the alignment groove at the desired axial position. If necessary, an insulated metal rod may be inserted into the ion collector block as an alternative detector.

2.4. Wafer processing

Prototypes were constructed for 320 μm OD capillaries with external conductive coatings. Variants with two different pupil widths (W_p = 200 μm and W_p = 300 μm) were fabricated. Standard 100 mm diameter, 550 μm thick (1 0 0) oriented, double-side polished Si wafers were first thermally oxidized at 1100 °C to form a 0.5 μm thick SiO_2 layer. The front side oxide was patterned using a UV mask aligner (IR 4000, Quintel Corp, San José, USA) using mask 1, and then etched using

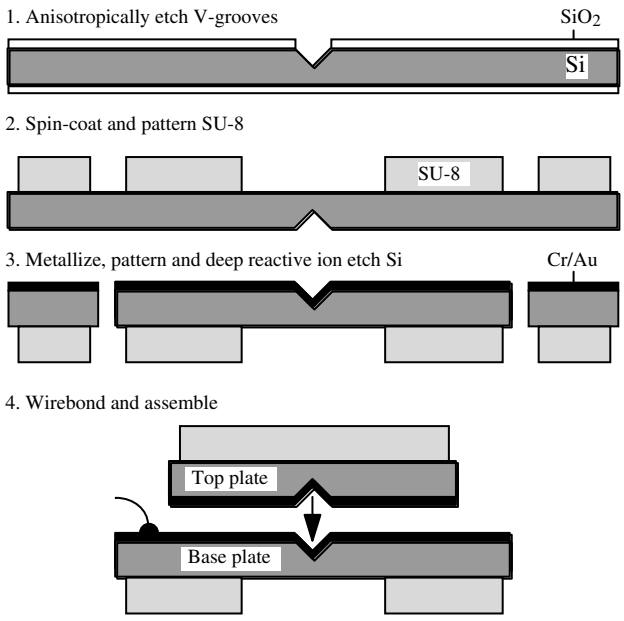

Figure 3. Process for fabrication of a microengineered nanospray alignment bench.

CHF_3, O_2 and Ar gases in a parallel plate reactive ion etcher (Plasmalab 80^+, Oxford Instruments, Bristol, UK) to define a hard mask. The silicon was then anisotropically etched to >200 μm depth using KOH.

After stripping residual oxide, a 300 μm thick layer of resist (SU-8 2100, Chestech, Rugby, UK) was spin coated on the rear side of the wafer and patterned using mask 2 to give a thick low-stress layer. The front side of the wafer was metallized with 300 Å Cr and 5000 Å Au metal using a vacuum coater (parallel-plate RF sputterer, Nordiko Technical Services, Havant, UK). Photoresist (Shipley Eagle 2100 ED, Chestech, UK) was deposited to form a conformal coating over the V-grooves, and patterned to define the electrodes. Exposed metal was removed by wet chemical etching, and the pattern was transferred right through the silicon using an inductively coupled plasma etcher (Surface Technology Systems, Newport, UK). At this point, the overall device structure consisted of isolated metallized silicon features on a plastic under-layer, which now formed the substrate. Residual resist and metal was then removed.

2.5. Die assembly

Dies were snapped out of the wafer by cleaving short sections of silicon material, with essentially 100% yield. Figure 4(*a*) shows a completed baseplate die. The crystal plane etch time has been chosen so that the groove forming the electrode pupil is etched to completion, while the capillary alignment groove is only partly formed. Base plate dies were mounted on small printed circuit boards and wirebonded. Top plate dies were then aligned under an optical microscope and fixed in place using conductive epoxy. Nanospray capillaries (silica tapertip, New Objective, Woburn, USA) were then inserted. Electrical connection to the exterior of the capillary is simply made by pressure contact between the microengineered mount and the conductive capillary coating. Replacement capillaries can be slid into place in a few minutes, and there is sufficient play to allow small variations in OD. Figure 4(*b*) shows a completed device.

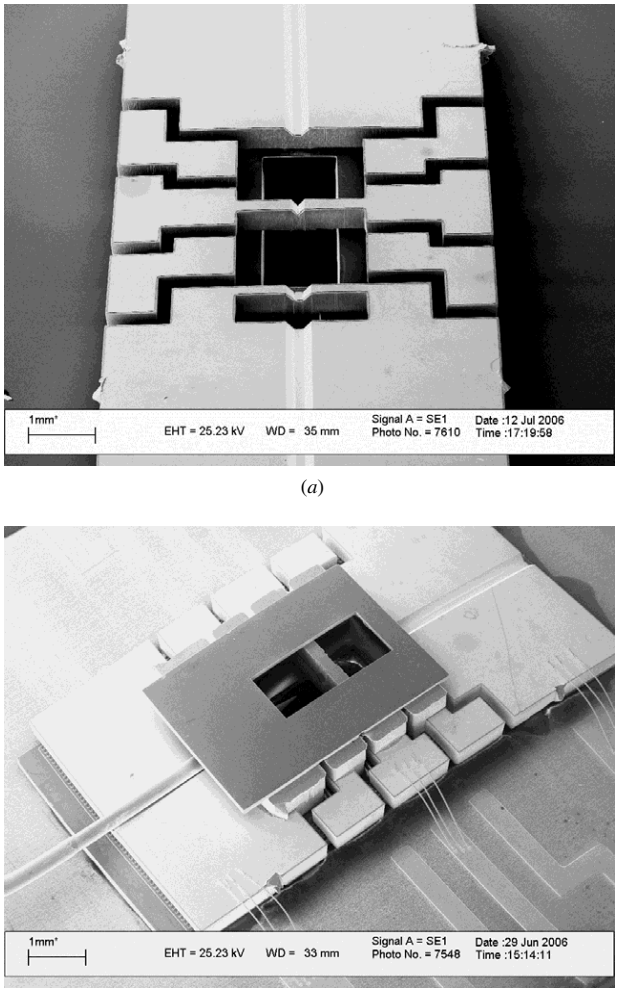

Figure 4. SEM views of (*a*) baseplate die and (*b*) an assembled nanospray alignment bench.

2.6. Initial assessment

The devices were mechanically robust. Despite the removal of most of the silicon, the dies were flat and it was not possible to detach the silicon from the plastic without breaking one of the two. Chemical durability (particularly, of the plastic base) was assessed, by immersing devices for 14 days in common electrospray solvents (water, dilute acetic acid, methanol and acetonitrile). No structural degradation was observed using either an optical microscope or a SEM. Electrical performance was also assessed, by applying a dc voltage between the capillary mount and the extraction electrode using a high voltage PSU (6515A, Hewlett Packard). Devices routinely withstood voltages >1200 V in air.

3. Results and discussion

3.1. Electrospray

For spray experiments, the nanospray capillary was connected to a 100 μm ID capillary line via a union (Upchurch Scientific,

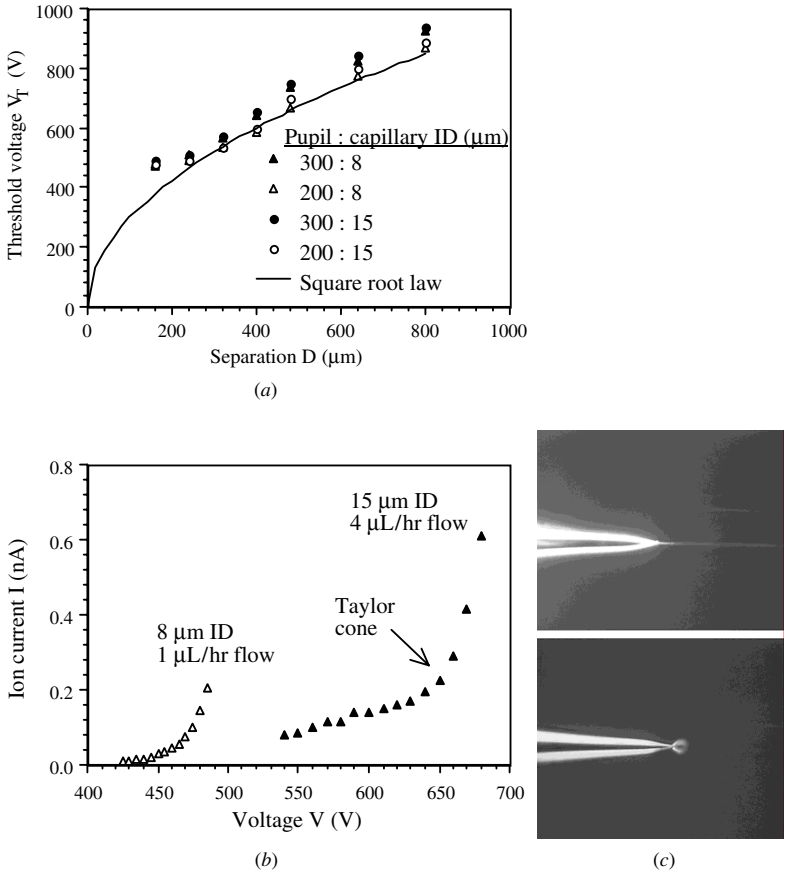

Figure 5. (*a*) Experimental variation of threshold voltage V_T with capillary-electrode separation D, for different capillary and pupil sizes (also shown is the theoretical square root law); (*b*) experimental variation of collected ion current I with voltage V, for different ID capillaries; (*c*) spray jets before and after Taylor cone formation. No nebulizer.

Oak Arbour, USA). Spray fluid (a 5%–20%–75% acetic acid—methanol–water mixture) was supplied using a syringe-pump (100-CE, KD Scientific, Holliston, USA) at flow rates in the range 1–40 μL h^{-1} (17–670 nL min^{-1}). The conductivity was determined using a commercial conductivity meter (HI-98130, Hanna Instruments, Leighton Buzzard, UK) as $\sigma = 0.7$ mS cm^{-1}. Voltages were arranged for positive ion production. Nebulizer gas was introduced by mounting the PCB on a Perspex substrate carrying a drilled gas line, so that gas passed through the PCB into the plenum and out through clearances between the V-groove and capillary. The capillary position and the spray were monitored using an optical microscope with a video camera and a cursor measurement system.

The design allowed accurate placement of the capillary tip at a prescribed axial separation from the extraction electrode. It was found that the syringe pump was required to fill the capillary line, but that spray would occur under voltage alone until the line was depleted. Once a spray had been initiated, it could be stopped and restarted electrically, and continuous spraying for several hours was demonstrated. The spray was generally axial, but off-axis and chaotic sprays were observed at very high voltages.

Nanospray was observed at low voltages. Figure 5(*a*) shows the variation of the threshold voltage V_T for Taylor cone formation with the separation D between the capillary tip and the extraction electrode, for nanospray capillaries with different internal diameters and pupils with different widths W_p. Here the flow rate Q is very low and no nebulizer gas is used. Larger voltages are required as the capillary ID, the pupil size and the separation between the capillary tip and the electrode are increased. However, spray initiation at below 500 V is clearly possible for both sizes of capillary, and V_T is less than 1 kV (standard for ESI) in all cases. The unusual shape of the electrode pupil makes detailed comparison with theory difficult. There is some evidence that the threshold voltage follows the theoretical law $V_T \sim D^{1/2}$ [3] (superimposed on one set of data) but the agreement deteriorates at separations approaching the pupil size.

Figure 5(*b*) shows measurements of the variation of the total ion current I with voltage V, for capillaries spaced 480 μm from an extraction electrode with a 300 μm pupil. Here an additional bias of 50 V was applied using the electrometer to ensure efficient ion collection. Data are shown for capillaries with two different IDs. Electrospray takes place only over a relatively small voltage range. The ion current increases quasi-linearly from zero at low voltage, but then rises much more rapidly. This behaviour was associated with two different types of spray, as shown in figure 5(*c*). At low voltages, emission was in the form of a pulsating 'droplet' at the capillary tip. A Taylor cone with an extended jet formed at a voltage corresponding to the knee of the *I*–*V* curve. A

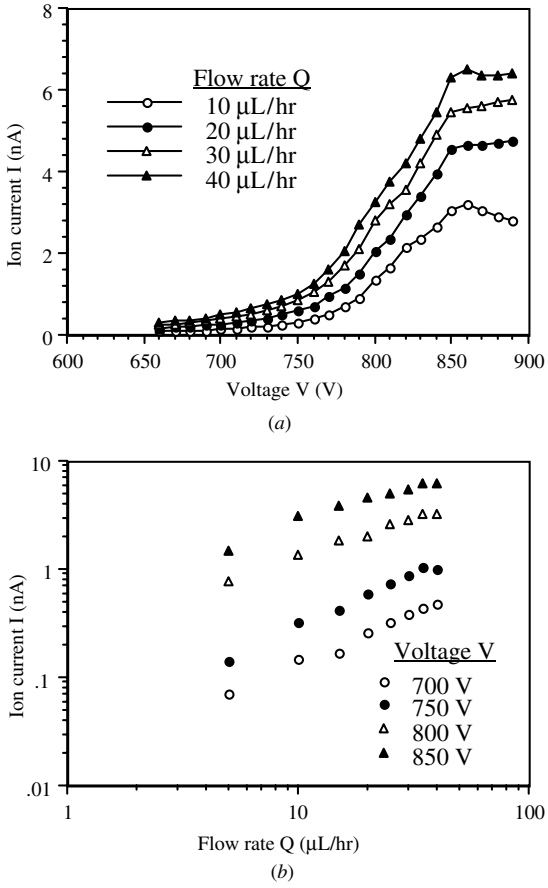

Figure 6. Experimental variation of collected ion current I with (*a*) voltage V, for different flow rates Q; (*b*) flow rate Q, for different voltages V. Nebulizer gas flowing.

larger threshold voltage is clearly required for the 15 μm ID capillary.

Larger currents were obtained using a nebulizer. The gas used was N_2 at 10 psi; however, it was difficult to quantify the flow because of leakage. Figure 6(*a*) shows the variation of the ion current I with the voltage V obtained using a nebulizer, for a 15 μm ID capillary spaced 480 μm from an extraction electrode with a 300 μm pupil. Data are shown for different flow rates; however, the flow rate appears to have little effect on the threshold voltage. The change in vertical axis scale from figure 5(*b*) should be noted. In each case, the ion current saturates at high voltage. Similar results were obtained with an insulated collector formed from a gold wire inserted into a capillary, suggesting that the spray is axial. Higher ion currents (up to 20 mA) were achieved with higher gas flows, but the current was less steady.

Figure 6(*b*) shows the variation of ion current with flow rate Q, for the 15 μm ID capillary above, at different fixed voltages V. The ion current varies as a power law of flow rate $I \sim Q^a$ [17] at low flow, again saturating at high rates. However, the exponent a appears to lie in the range $1/2 \leqslant a \leqslant 1$, rather than simply being fixed at $a = 1/2$. Lower ion currents (3 nA) were achieved from smaller capillaries, at lower voltages (600 V). Experiments were also carried out using larger (30 μm ID) capillaries, and ion currents of 16 nA were achieved at 1.2 kV.

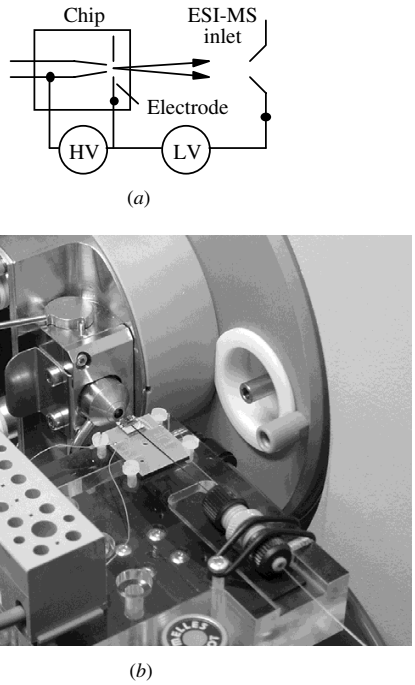

Figure 7. Arrangement for use with an ESI mass spectrometer: (*a*) schematic and (*b*) actual.

3.2. Mass spectrometry

Mass spectrometry was carried out using a ZQ Micromass ESI mass spectrometer (Waters Corp., Milford, USA). The existing electrospray source was removed, and a nanospray source (without an on-chip ion collector) was mounted directly in front of the sampling cone on a three-axis stage, as shown in figures 7(*a*) and (*b*). The nanospray source can be seen mounted on a small PCB at the centre of the photograph. The analyte was a calibration solution of NaI and CsI in water and IPA, and the flow rate was 7 μL h^{-1}. A 15 μm ID nanospray capillary was used, with N_2 nebulizer gas. Spray initiation was detected by monitoring the current on the extraction electrode. Approximately 100 nA was measured at a voltage of 800 V. The combination of a small (50 V) dc voltage and the drag of the inlet gas was used to couple ions into the ZQ. No feedback was used to stabilize the ion signal. Figure 8(*a*) shows a mass spectrum obtained with no drying gas or heating of the ZQ vacuum interface, together with example peak assignments. Similar, desolvated spectra were obtained with drying and heating applied.

The ion current measured on the ZQ sampling cone was extremely stable, and insensitive to the exact position of the spray chip, which could be realigned manually while measurements were carried out. Figure 8(*b*) shows the variation of the total ion current (TIC) and the current obtained at the highest mass peak, 132.9 amu (Cs^+), under different conditions. Initially (point A), the source was located on axis, 3.2 mm from the sampling cone. After 10 min (point B), the source was moved axially by 2 mm, so that it now lay 5.2 mm away. There is little reduction in signal strength, but some improvement in signal-to-noise ratio. After 20 min (point C), it was moved 2 mm off axis in the vertical direction, and after

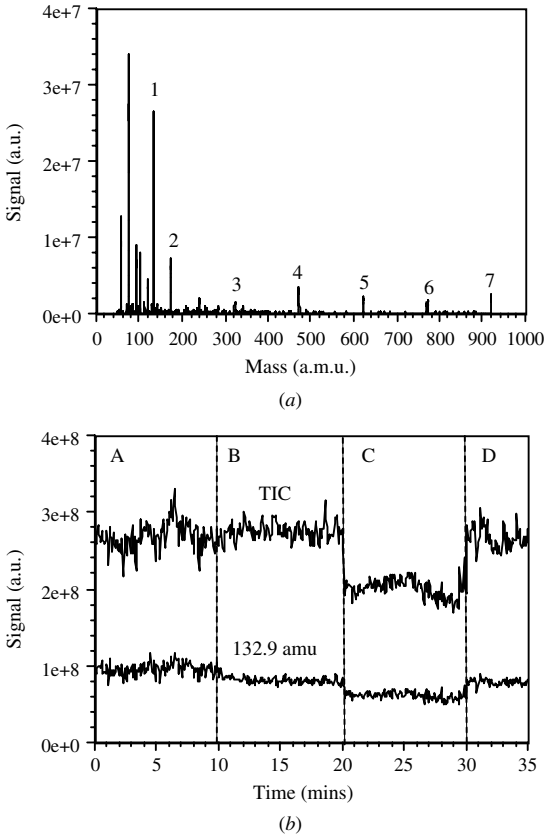

Figure 8. (*a*) Mass spectrum for NaI/CsI calibration solution (1—Cs^+; 2—$Na(NaI)^+$; 3—$Na(NaI)_2^+$; 4—$Na(NaI)_3^+$; 5—$Na(NaI)_4^+$; 6—$Na(NaI)_5^+$; 7—$Na(NaI)_6^+$); (*b*) variation of total and selected ion current with time during stability experiments.

30 minutes (point D), a further 2 mm off axis in the horizontal direction. In each case, there was no difficulty in obtaining a signal, and the signal stabilized immediately.

In contrast, ion currents obtained with a bare nanospray capillary depended strongly on the exact position of the capillary with respect to the ESI-MS, and were extremely unstable. The main reasons for the improved performance of the chip-based system are shielding of the field generated by the ESI-MS from the capillary by the ion extraction electrode, and the use of a small, well-controlled volume for nebulization.

4. Conclusions

We have developed a novel miniaturized system for passive alignment of nanospray capillaries, based on a microengineered breadboard that locates the capillary accurately with respect to an on-chip ion extraction electrode and allows axial spray at well-defined voltages. The device combines V-shaped alignment features and a diaphragm electrode formed in metallized silicon with a plastic base formed in thick photopatterned resist. Fabrication is carried out on standard silicon wafers using a batch process. The process is extremely flexible and has the potential to allow other electrode arrangements, for example for deflection of the spray. These electrodes may be provided without additional cost.

The alignment bench is mechanically and chemically robust. The plastic substrate provides excellent electrical isolation and contains features for gas injection and drainage. Electrical characterization has been carried out over a range of capillary diameters using devices with an on-chip ion collector. The system sprays at low voltage and has operated reliably over extended periods. ESI-MS experiments have been carried out with an atmospheric pressure ionization mass spectrometer. Stable ion currents are achieved, and the signal is only weakly dependent on the source position with respect to the sampling cone.

Acknowledgments

The authors are very grateful to the Department of Trade and Industry for funding under the Technology Program Project 'IONCHIP' and to GSK Ltd for their loan of the ZQ Micromass system. The contribution of Mr Alan Finlay of Microsaic Systems Ltd in providing much of the impetus of this work is also gratefully acknowledged.

References

[1] Dole M, Mack L L, Hines R L, Mobley R C, Ferguson L D and Alice M B 1968 Molecular beams of macroions *J. Chem. Phys.* **49** 2240–9
[2] Yamashita M and Fenn J B 1984 Electrospray ion source: another variation on the free-jet theme *J. Phys. Chem.* **88** 4451–9
[3] Wilm M and Mann M 1994 Electrospray and Taylor-cone theory, Dole's beam of macromolecules at last? *Int. J. Mass Spectrosc. Ion Proc.* **136** 167–80
[4] Gale D C and Smith R D 1993 Small volume and low flow-rate electrospray ionization mass spectrometry of aqueous samples *Rapid Commun. Mass Spectrosc.* **7** 1017–21
[5] Wilm M and Mann M 1996 Analytical properties of the nanoelectrospray ion source *Anal. Chem.* **68** 1–8
[6] Warriner R N, Craze A S, Games D E and Lane S J 1998 Capillary electrochromatography mass spectrometry—a comparison of the sensitivity of nanospray and microspray ionization techniques *Rapid Commun. Mass Spectrosc.* **12** 1143–9
[7] Juraschek R, Dülcks T and Karas M 1999 Nanoelectrospray—more than just a minimized-flow electrospray ionization source *J. Am. Soc. Mass Spectrosc.* **10** 300–8
[8] Gelpi E 2002 Interfaces for coupled liquid-phase separation/mass spectrometry techniques: an update on recent developments *J. Mass Spectrosc.* **37** 241–53
[9] Wood T D, Moy M A, Dolan A R, Bigwarfe P M, White T P, Smith D R and Higbee D J 2003 Miniaturization of electrospray ionization mass spectrometry *Appl. Spectrosc. Rev.* **38** 187–244
[10] Schmitt-Kopplin P and Frommberger M 2003 Capillary electrophoresis—mass spectrometry: 15 years of developments and applications *Electrophoresis* **24** 3837–67
[11] Zeleny J 1917 Instability of electrified liquid surfaces *Phys. Rev.* **10** 1–6
[12] Taylor G I 1964 Disintegration of water drops in an electric field *Proc. R. Soc.* A **280** 383–97
[13] Cloupeau M and Prunet-Foch B 1989 Electrostatic spraying of liquids in cone-jet mode *J. Electrostat.* **22** 135–59
[14] Ganan-Calvo A M 1997 Cone-jet analytical extension of Taylor's electrostatic solution and the asymptotic universal scaling laws in electrospraying *Phys. Rev. Lett.* **79** 217–20

[15] Higuera F J 2004 Current/flow-rate characteristic of an electrospray with small meniscus *J. Fluid Mech.* **513** 239–46
[16] De La Mora J F 1992 The effect of charge emission from electrified liquid cones *J. Fluid Mech.* **243** 561–74
[17] De La Mora F J and Loscertales I G 1994 The current emitted by highly conducting Taylor cones *J. Fluid Mech.* **260** 155–84
[18] Lundqvist A, Pihl J and Orwar O 2000 Tantalum-filament pulling device for fabrication of submicrometer fused silica tips *Anal. Chem.* **72** 5740–3
[19] Hannis J C and Muddiman D C 1998 Nanoelectrospray mass spectrometry using nonmetallized, tapered (50 → 10 μm) fused silica capillaries *Rapid Commun. Mass Spectrosc.* **12** 443–8
[20] Kriger M S, Cook K D and Ramsey R S 1995 Durable gold-coated fused silica capillaries for use in electrospray mass spectrometry *Anal. Chem.* **67** 385–9
[21] Valaskovic G A 1996 Long-lived metalized tips for nanolitre electrospray mass spectrometry *J. Am. Soc. Mass Spectrosc.* **7** 1270–2
[22] Marziarz E P I, Lorenz S A, White T P and Wood T D 2000 Polyaniline: a conductive polymer coating for durable nanospray emitters *J. Am. Soc. Mass Spectrosc.* **11** 659–63
[23] Nilsson S, Wetterhall M, Bergquist J, Nyholm L and Markides K E 2001 A simple and robust conductive graphite coating for sheathless electrospray emitters used in capillary electrophoresis/mass spectrometry *Rapid Commun. Mass Spectrosc.* **15** 1997–2000
[24] Smith D R, Moy M A, Dolan A R and Wood T D 2006 Analytical performance characteristics of nanoelectrospray emitters as a function of conductive coating *Analyst* **131** 547–55
[25] Valaskovic G A, Murphy J P and Lee M S 2004 Automated orthogonal control system for electrospray ionization *J. Am. Soc. Mass Spectrosc.* **15** 1201–15
[26] Ramsey R and Ramsey J 1997 Generating electrospray from microchip devices using electroosmotic pumping *Anal. Chem.* **69** 1174–8
[27] Figeys D, Ning Y B and Aebersold R 1997 A microfabricated device for rapid protein identification by microelectrospray ion trap mass spectrometry *Anal. Chem.* **69** 3153–60
[28] Licklider L, Wang X Q, Desai A, Tai Y C and Lee T D 2000 A micromachined chip-based electrospray source for mass spectrometry *Anal. Chem.* **15** 367–75
[29] Kim J-S and Knapp D R 2001 Miniaturized multichannel electrospray ionization emitters on poly(dimethylsiloxane) microfluidic devices *Electrophoresis* **22** 3993–9
[30] Chen S-H, Sung W C, Li G-B, Lin Z-Y, Chen P-W and Liao P-C 2001 A disposable poly(methylmethacrylate)-based microfluidic module for protein identification by nanoelectrospray ionization-tandem mass spectrometry *Electrophoresis* **22** 3972–7
[31] Svedberg M, Petterson A, Nilsson S, Bergquist J, Nyholm L, Nikolajeff F and Markides K 2003 Sheathless electrospray from polymer microchips *Anal. Chem.* **75** 3934–40
[32] Kameoka J, Orth R, Ilic B, Czaplewski D, Wachs T and Craighead H G 2002 An electrospray ionization source for integration with microfluidics *Anal. Chem.* **74** 5897–901
[33] Legrand B, Ashcroft A E, Buchaillot L and Arscott S 2007 SOI-based nanoelectrospray emitter tips for mass spectrometry: a coupled MEMS and microfluidic design *J. Micromech. Microeng.* **17** 509–14
[34] Le Gac S, Arscott S and Rolando C 2003 A planar microfabricated nanoelectrospray emitter tip based on a capillary slot *Electrophoresis* **24** 3640–7
[35] Kim M-S, Joo H-S, Kim B-G and Kim Y-K 2006 A microfabricated device with integrated nanoelectrospray source for capillary electrophoresis and mass spectrometry *SPIE Proc.* **6036** 369–76
[36] Sen A K, Darabi J, Knapp D R and Liu J 2006 Modeling and characterization of a carbon fiber emitter for electrospray ionization *J. Micromech. Microeng.* **16** 620–30
[37] Sen A K, Darabi J and Knapp D R 2007 Simulation and parametric study of a novel multi-spray emitter for ESI-MS applications *Microfluid. Nanofluid.* **3** 283–98
[38] Sjoedahl J, Melin J, Griss P, Emmer A, Stemme G and Roerade J 2003 Characterization of micromachined hollow tips for two-dimensional nanoelectrospray mass spectrometry *Rapid Commun. Mass Spectrosc.* **17** 337–41
[39] Schultz G A, Corso T N, Prosser S J and Zhang S 2000 A fully integrated monolithic microchip electrospray device for mass spectrometry *Anal. Chem.* **72** 4058–63
[40] Corkery L J, Pang H, Schneider B B, Covey T R and Siu K W M 2005 Automated nanospray using chip-based emitters for the quantitative analysis of pharmaceutical compounds *J. Am. Soc. Mass Spectrosc.* **16** 363–9
[41] Franssila S, Marttila S, Kolari K, Ostman P, Kotiaho T, Kostiainen R, Lehtiniemi R, Fager C-M and Manninen J 2006 A microfabricated nebulizer for liquid vaporization in chemical analysis *J. Microelectromech. Syst.* **15** 1251–9
[42] Sung W-C, Makamba H and Chen S-H 2005 Chip-based microfluidic devices coupled with electrospray ionization-mass spectrometry *Electrophoresis* **26** 1783–91
[43] Lee D B 1969 Anisotropic etching of silicon *J. Appl. Phys.* **40** 4569–74
[44] Petersen K E 1982 Silicon as a mechanical material *Proc. IEEE* **70** 420–57
[45] Schroeder C M 1977 Accurate silicon spacer chips for an optical fiber cable connector *Bell. Syst. Tech. J.* **57** 91–7
[46] Hillerich B and Geyer A 1988 Self-aligned flat-pack fibre-photodiode coupling *Elect. Lett.* **24** 918–19
[47] Hynes A M, Ashraf H, Bhardwaj J K, Hopkins J, Johnston I and Shepherd J N 1999 Recent advances in silicon etching for MEMS using the ASE^{TM} process *Sensors Actuators* **74** 13–7
[48] Kersten P, Bouwstra S and Petersen J W 1995 Photolithography on micromachined 3D surfaces using electrodeposited photoresists *Sensors Actuators* A **51** 51–4
[49] Conradie E H and Moore D F 2002 SU-8 thick photoresist processing as a functional material for MEMS applications *J. Micromech. Microeng.* **12** 368–74
[50] Geear M, Syms R R A, Wright S and Holmes A S 2005 Monolithic MEMS quadrupole mass spectrometers by deep silicon etching *IEEE/ASME J. Microelectromech. Syst.* **14** 1156–66